VALIDATION OF CIVA 10 RT MODULE IN A NUCLEAR CONTEXT, FOR DISSIMILAR METAL WELD

D. Tisseur[1], B. Rattoni[1], F. Buyens[1], G. Cattiaux[2], T. Sollier[2]
[1]CEA LIST, CEA Saclay 91191 Gif sur Yvette Cedex, France
[2]IRSN/PSN-EXP/SES, B.P.17 92262 Fontenay-Aux-Roses Cedex, France

ABSTRACT
CIVA platform is a non-destructive testing software developed by CEA LIST which integrates an X-ray/gamma ray radiography module. For several years, a research program funded by the French Institute for Radiological Protection and Nuclear Safety (IRSN) studies gamma/X-ray simulation tools for evaluating NDE methods in the nuclear context. In this framework, IRSN, in partnership with CEA LIST, started in 2010 a program lasting several years for the validation of CIVA RX module. In 2011, a preliminary study has been performed on a dissimilar metal weld mockup representative of a weld of a primary piping in a nuclear power plant. The mock up presents large notches with a thickness of 0.2 mm and a height of 3 and 5 mm. This preliminary study has shown a good accuracy between CIVA and experimental results. To complete this study, six notches with several sizes (6 mm height and from 20 µm to 150 µm opening), orientations (axial or circumferential) and positions have been superimposed to the weld thanks to a manufactured insert. This study presents validation results for ^{192}Ir and ^{60}Co gamma sources.

Keywords: Radiography, gamma source, validation, Monte Carlo simulation, CIVA **PACS:** 28.41.Ak

INTRODUCTION
NDE techniques are used mainly during inspection of nuclear components for maintenance operations. For safety reasons, we need to know the performances of these NDE techniques. The simulation can be a powerful tool to evaluate the performances of NDE techniques in complement with experimental acquisition on mock-ups. The CIVA software integrates a gamma and x-ray radiography module [1-3] that has been developed in collaboration between CEA LETI (Monte Carlo computation and direct beam fusion, detector models) [4-5], EDF (ray tracing and Monte Carlo implementations, detector models) [6,7,10], CEA LIST (GUI, tomography), and IRSN (validation, case study on realistic nuclear component from various nuclear facilities) [8].

A few years ago, a research program funded by the French Institute for Radioprotection and Nuclear Safety (IRSN) was initiated to study the benefits of X-Ray simulation tools for the assessment of NDE methods used on nuclear components.

In this context, since 2009, IRSN has launched a large validation study of CIVA RX module. A preliminary validation study has been performed in 2011 on a dissimilar metal weld mock-up on large notches with cobalt 60 gamma source [16]. For this validation, we have used 3 notches with a length of 20 mm, an opening of 0.2 mm and a height of 5 mm and 3 notches with a length of 20 mm, an opening of 0.2 mm and a height of 3 mm. The cross comparison between simulation performed with CIVA 10 radiography module and experimental data have shown a good accuracy between simulation and experimental x-ray film.

MATERIALS AND METHODS
For this study, we used CIVA 10 version. Given the context of thick components, we used the fusion approach of scattered and transmitted images respectively from Monte Carlo and analytical computations to simulate the final images [3,4,5]. The number of photons used in the scattering simulation has been chosen to be in conformity with the required number [4]. The detector model (Gray model [11]) developed

by EDF [10,12] is based on the European standard EN 584-1 [9] and converts the incident dose into an optical density value. A decomposition of a volumic source into several small source points [6] allowed the simulation of the source blurring. For this study, the source has been decomposed into 20 sources point.

We used a dissimilar weld mock-up representative of typical nuclear component. This mock-up is composed on one side of 16MND5 alloy side and on the other side of a 316L alloy (see figure 1).

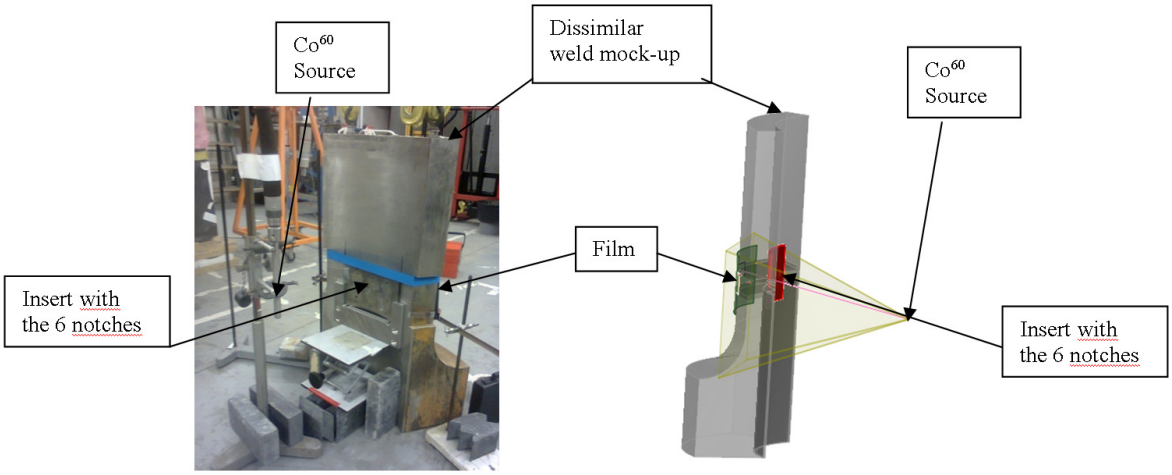

Figure 1: On the left, the experimental set up. On the right, the CIVA simulation set-up

Six notches with several sizes (a height of 6 mm and an opening from 20 µm to 150 µm), orientations (axial or circumferential) and positions have been superimposed to the weld thanks to a manufactured insert (see figure 2 and table 1).

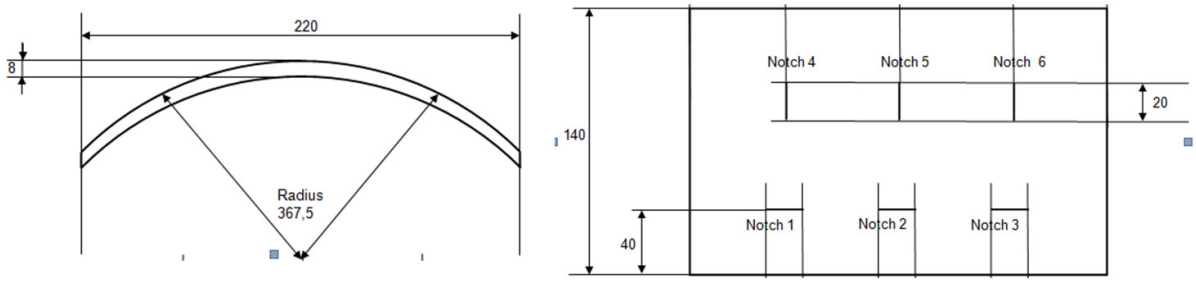

Figure 2: Schema of the insert with the 6 notches.

Reference	Name	Length (mm)	Height (mm)	Opening (mm)
Notch 1	C1E1-6-20	20	6	0.020
Notch 2	C1E2-6-40	20	6	0.040
Notch 3	C1E3-6-60	20	6	0.060
Notch 4	C1E4-6-80	20	6	0.080
Notch 5	C1E5-6-100	20	6	0.100
Notch 6	C1E6-6-150	20	6	0.150

Table 1: Description of the six notches.

For this validation, the notches are positioned in a circumferential and a longitudinal configuration (see figure 3 and 4). For each configuration, the notches are moved into three positions:

- Position A (axed on the weld): The notches are positioned circumferentially or axially on the middle of the weld.

- Position B (shifted on the stainless steel side) : The notches are positioned circumferentially or axially on the axe of the buttering on the ferritic side

- Position C (shifted on the ferritic steel side) : The notches are positioned circumferentially or axially on the axe of the buttering on the stainless steel side

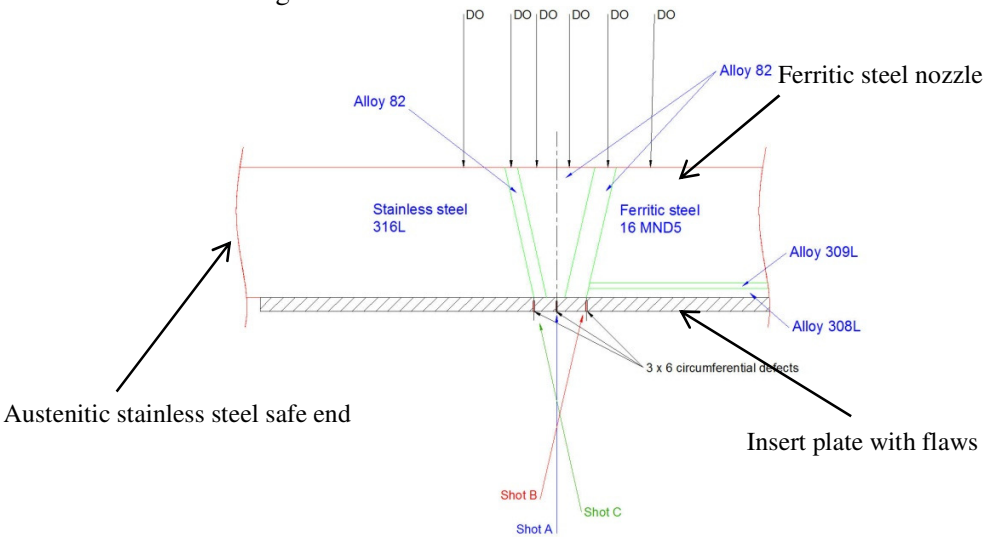

Figure 3: Set-up of the circumferential configuration

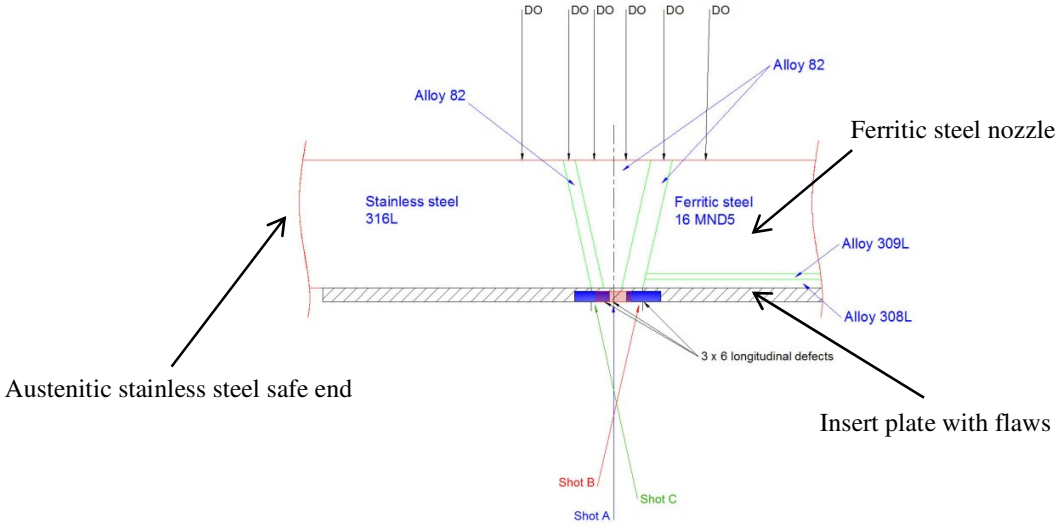

Figure 4: Set-up of the longitudinal configuration

We used a Co^{60} gamma source with a diameter of 3.7 mm and a height of 3.7 mm and an Ir^{192} gamma source with a diameter of 3 mm and a height of 3 mm. We used M100 Kodak x-ray films, manually developed in conformity with Kodak recommendations. The distance from the source to the mock-up is 0.367 m. Filters and reinforced used screens are in conformity with the French Regulatory requirements and design code (RCC-M) and European standard [13,14,15]. The films are digitized with a Ge FS50B scanner with a pixel size of 50 µm x 50 µm.

RESULTS AND DISCUSSIONS

Validation with Co60 gamma source

Figure 5 presents optical density profiles comparison between CIVA and experimental film perpendicularly to the weld. The simulated data agrees with the experimental data.

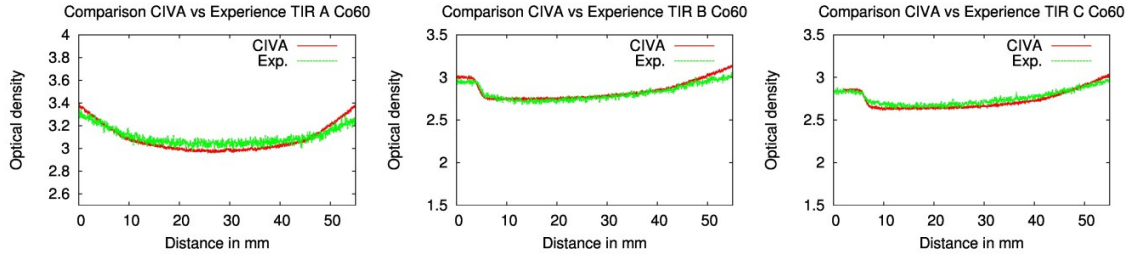

Figure 5: On the left, optical density profile comparison between CIVA and the experimental image for the source in position A. On the middle, optical density profile comparison between CIVA and the experimental image for the source in position B. On the right, optical density profile comparison between CIVA and the experimental image for the source in position C

Optical density profiles have been extracted from the several images on the different notches (see figure 6). Amplitude and width at middle height have been measured on each notch on experimental and simulated images.

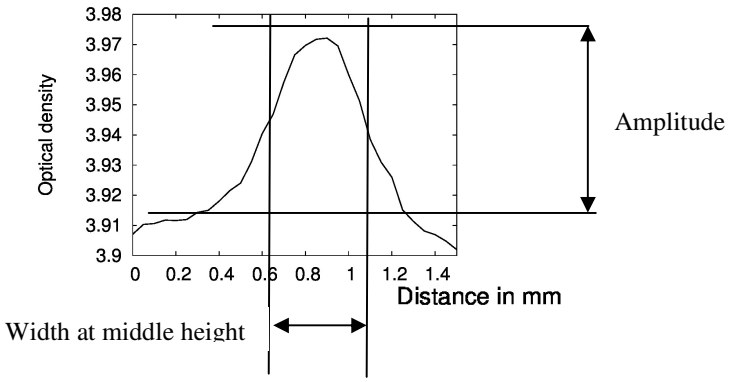

Figure 6: Measure of the amplitude and width at middle height.

The following table shows the results (note that ND= none detected).

	Flaw	Measured amplitude	Simulated amplitude	Measured width at middle height in mm	Simulated width at middle height in mm
Position A circumferential flaw	C1E1-6-20	0.007	0.005	0.60	0.74
	C1E2-6-40	0.014	0.011	0.99	0.85
	C1E3-6-60	0.018	0.010	0.70	0.84
	C1E4-6-80	0.023	0.019	0.75	0.83
	C1E5-6-100	0.035	0.025	0.78	0.88
	C1E6-6-150	0.047	0.035	0.79	0.91
Position A longitudinal flaw	C1E1-6-20	0.006	0.005	0.52	0.47
	C1E2-6-40	0.009	0.009	0.69	0.72
	C1E3-6-60	0.016	0.012	0.97	0.71
	C1E4-6-80	0.021	0.020	0.91	0.85
	C1E5-6-100	0.021	0.022	0.87	0.82
	C1E6-6-150	0.036	0.036	0.91	0.84

Table 2: Amplitude and width comparison between CIVA and experimental data on the 6 notches for circumferential and longitudinal positions for the position A of the source.

	Flaw	Measured amplitude	Simulated amplitude	Measured width at middle height in mm	Simulated width at middle height in mm
Position B circumferential flaw	C1E1-6-20	ND	ND	ND	ND
	C1E2-6-40	ND	ND	ND	ND
	C1E3-6-60	ND	ND	ND	ND
	C1E4-6-80	0.013	0.010	1.54	1.36
	C1E5-6-100	0.015	0.012	1.65	1.43
	C1E6-6-150	0.022	0.018	1.69	1.57
Position B longitudinal flaw	C1E1-6-20	0.008	0.008	0.89	0.99
	C1E2-6-40	0.011	0.012	0.98	0.92
	C1E3-6-60	0.020	0.015	0.92	0.81
	C1E4-6-80	0.022	0.024	0.99	0.90
	C1E5-6-100	0.033	0.030	1.00	0.89
	C1E6-6-150	0.042	0.042	0.99	0.88

Table 3: Amplitude and width comparison between CIVA and experimental data on the 6 notches for circumferential and longitudinal positions for the position B of the source.

	Flaw	Measured amplitude	Simulated amplitude	Measured width at middle height in mm	Simulated width at middle height in mm
Position C circumferential flaw	C1E1-6-20	ND	ND	ND	ND
	C1E2-6-40	ND	ND	ND	ND
	C1E3-6-60	ND	ND	ND	ND
	C1E4-6-80	ND	ND	ND	ND
	C1E5-6-100	ND	ND	ND	ND
	C1E6-6-150	ND	ND	ND	ND
Position C longitudinal flaw	C1E1-6-20	0.005	0.003	1.13	0.87
	C1E2-6-40	0.007	0.008	1.04	0.98
	C1E3-6-60	0.012	0.011	1.09	0.95
	C1E4-6-80	0.019	0.017	0.95	0.89
	C1E5-6-100	0.022	0.021	0.98	0.95
	C1E6-6-150	0.032	0.030	1.01	0.91

Table 4: Amplitude and width comparison between CIVA and experimental data on the 6 notches for circumferential and longitudinal positions for the position C of the source.

The comparisons between CIVA and experimental data show a good adequacy. The maximal errors are observed in high optical density gradient (position B and C) due to the measuring difficulty. However, all the flaws detected on the radiographic film are detected on the simulated film. The non-detected flaws on the simulation are not detected on the radiographic film. For the B and C position with circumferential flaw, the smallest notches are not detected because there are in an area with an important optical density gradient. The absolute error in term of optical density are more important for the B and C position (influence of scattered beam, the ratio between direct and scattered beam is more important).

The maximal errors are observed for the smallest flaws. The comparisons show that the simulation tends to underestimate the flaw amplitude and over-estimate the flaws width. The effects are probably due to the modulation transfer function estimation (response on the film)

Validation with Ir192 gamma source

Figure 5 presents optical density profiles comparison between CIVA and experimental film. The simulated data agrees with the experimental data. The maximum relative error (figure 5) is observed for the source position B. This error is probably due to the scattered beam due the massive ferritic part of the mock-up.

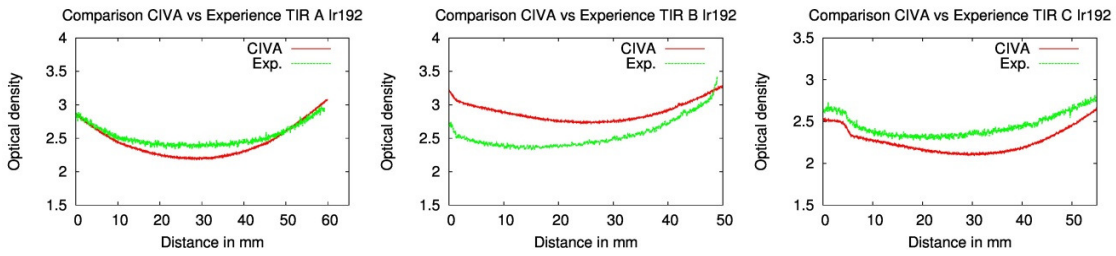

Figure 5: On the left, optical density profile comparison between CIVA and the experimental image for the source in position A. On the middle, optical density profile comparison between CIVA and the

experimental image for the source in position B. On the right, optical density profile comparison between CIVA and the experimental image for the source in position C

Optical density profiles have been extracted from the several images on the different notches. Amplitude and width at middle height have been measured on each notch on experimental and simulated images. The following table shows the results.

	Flaw	Measured amplitude	Simulated amplitude	Measured width at middle height in mm	Simulated width at middle height in mm
Position A circumferential flaw	C1E1-6-20	0.011	0.008	0.53	0.55
	C1E2-6-40	0.011	0.010	0.51	0.52
	C1E3-6-60	0.013	0.013	0.69	0.71
	C1E4-6-80	0.025	0.015	0.61	0.64
	C1E5-6-100	0.031	0.018	0.67	0.61
	C1E6-6-150	0.041	0.020	0.61	0.63
Position A longitudinal flaw	C1E1-6-20	ND	ND	ND	ND
	C1E2-6-40	0.011	0.010	0.61	0.55
	C1E3-6-60	0.014	0.011	0.62	0.58
	C1E4-6-80	0.025	0.016	0.58	0.57
	C1E5-6-100	0.030	0.019	0.65	0.61
	C1E6-6-150	0.042	0.028	0.69	0.62

Table 5: Amplitude and width comparison between CIVA and experimental data on the 6 notches for circumferential and longitudinal positions for the position A of the source.

	Flaw	Measured amplitude	Simulated amplitude	Measured width at middle height in mm	Simulated width at middle height in mm
Position B circumferential flaw	C1E1-6-20	ND	ND	ND	ND
	C1E2-6-40	ND	ND	ND	ND
	C1E3-6-60	ND	ND	ND	ND
	C1E4-6-80	0.002	0.005	1.31	1.44
	C1E5-6-100	0.009	0.007	1.44	1.38
	C1E6-6-150	0.026	0.021	1.65	1.67
Position B longitudinal flaw	C1E1-6-20	0.008	0.005	0.56	0.59
	C1E2-6-40	0.016	0.010	0.61	0.58
	C1E3-6-60	0.020	0.015	0.64	0.61
	C1E4-6-80	0.024	0.021	0.61	0.68
	C1E5-6-100	0.035	0.026	0.59	0.69
	C1E6-6-150	0.050	0.032	0.62	0.64

Table 6: Amplitude and width comparison between CIVA and experimental data on the 6 notches for circumferential and longitudinal positions for the position B of the source.

	Flaw	Measured amplitude	Simulated amplitude	Measured width at middle height in mm	Simulated width at middle height in mm
Position B circumferential flaw	C1E1-6-20	ND	ND	ND	ND
	C1E2-6-40	ND	ND	ND	ND
	C1E3-6-60	ND	ND	ND	ND
	C1E4-6-80	ND	ND	ND	ND
	C1E5-6-100	ND	ND	ND	ND
	C1E6-6-150	ND	ND	ND	ND
Position B longitudinal flaw	C1E1-6-20	0.009	0.008	0.52	0.56
	C1E2-6-40	0.012	0.015	0.59	0.67
	C1E3-6-60	0.018	0.019	0.59	0.53
	C1E4-6-80	0.023	0.027	0.64	0.56
	C1E5-6-100	0.035	0.035	0.67	0.59
	C1E6-6-150	0.046	0.045	0.58	0.59

Table 7: Amplitude and width comparison between CIVA and experimental data on the 6 notches for circumferential and longitudinal positions for the position C of the source.

The comparisons between CIVA and experimental data show a good agreement. The maximal errors are observed in high optical density gradient (position B and C) due to the measuring difficulty. However, all the flaws detected on the radiographic film are detected on the simulated film. The non-detected flaws on the simulation are not detected on the radiographic film. For the B position with circumferential flaw, the smallest notches are not detected because there are in an area with an important optical density gradient.

For the C position with circumferential flaw, the flaws are detected with a lot of difficulties. There is an important uncertainty to say if the flaws are detected. The absolute errors in term of optical density are less important for the ^{60}Co source in comparison with ^{192}Ir source. The maximal errors are observed for the smallest flaws. The comparisons show that the simulation tends to underestimate the amplitude and the width of the flaws. The effects are probably due to the modulation transfer function estimation (response on the film).

CONCLUSIONS AND PERSPECTIVES

Specific validations have shown that:

- The results obtained for ^{60}Co and ^{192}Ir gamma sources show a good accuracy between experiment and simulation with an EN584-1 film model.
- Results show the importance of detector modulation transfer function in the simulation.

The next step of this study will be the validation of CIVA 10 for a cast stainless steel mock-up with gamma source and complex mock-up with x-ray tube. Experiments will be performed and compared to simulations.

REFERENCES

1. http://www-civa.cea.fr
2. R. Fernandez, A. Schumm, J. Tabary, P. Hugonnard, “Simulation studies of radiographic inspections with CIVA”, in 17th WCNDT, Shanghai (2008).
3. J. Tabary, P. Hugonnard, A. Schumm, R. Fernandez “Simulation studies of radiographic inspections with Civa", in COFREND 2008

4. R. Guillemaud, J. Tabary, P. Hugonnard, F. Mathy, A. Koenig, A. Glière, "SINDBAD: a multipurpose and scalable X-Ray simulation tool for NDE and medical imaging", in PSIP 2003, Grenoble, France (2003).
5. J. Tabary, F. Mathy, P. Hugonnard "New Functionalities in “SINDBAD” Software for Realistic X-Ray Simulation Devoted to Complex Parts Inspection" , in ECNDT 2006
6. A. Schumm, O. Bremnes, B. Chassignole, "Numerical simulation of radiographic inspection: fast and realistic results even for thick components", in Proceedings of the 16th world conference of Non-Destructive Testing, Montreal (2004)
7. O. Bremnes, B. Chassignole, O. Dupond, A. Schumm, "Experimental And Simulation Studies Of Radiographic Inspections Of Pressure Vessel Reactors" in ECNDT London 2006
8. F. Mathy, C. Poidevin, G. Cattiaux, T. Sollier “Radiographic testing simulation with CIVA-RX – assessment on representative nuclear components”, in ECNDT Moscow 2010
9. EN 584-1:2006, "Non-destructive testing – Industrial radiographic film – Part 1: Classification of film systems for industrial radiography", European standard for non-destructive evaluation
10. A. Schumm, U. Zscherpel, “The EN584 standard for the classification of industrial radiography films and its use in radiographic modeling”, in Proceedings of the Sixth International Conference on NDE in relation to structural integrity for nuclear and pressurized components (2007).
11. T.Jensen, T.Aljundi, J.N.Gray, and R.Wallingford, “A model of X-ray film response”, in Review of progress in Quantitative Nondestructive Evaluation, edited by D. O. Thompson and D. E. Chimenti, AIP Conference Proceedings, American Institute of Physics, Melville, NY Vol 15, pp441-448 (1996).
12. A. Schumm, U. Zscherpel, “Radiographic film modeling according to EN584”, in *COFREND 2008*
13. EN 444:1994, “Non-destructive testing — General principles for Radiographic examination of metallic materials by X- and gamma-rays”, European standard for non-destructive evaluation
14. RCC-M :2007, “Regulatory requirements and design code”, AFCEN publication
15. NF EN 13068-1:2000, “Radioscopic testing - Part 1 : quantitative measurement of imaging properties.”, European standard for non-destructive testing
16. D. Tisseur, F. Buyens, B. Rattoni, G. Cattiaux, T. Sollier, “CIVA 10 RT module: preliminary validation in a nuclear context“, in Review of progress in Quantitative Nondestructive *Evaluation*, edited by D. O. Thompson and D. E. Chimenti, AIP Conference Proceedings, American Institute of Physics, Melville, NY Proceedings (QNDE '11), 2011